

Investigation of the effects of non-linear glucose kinetics in hypo- and hyperglycaemic states

Doctoral (PhD) thesis

Zsófia Ragoncsa Gáborné Nagy MD

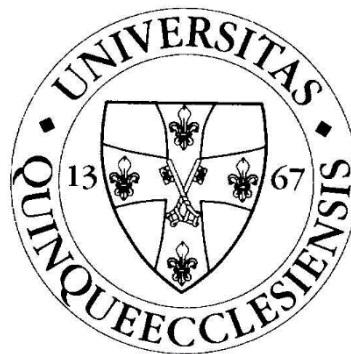
Clinical Medical Sciences

Leader of the Doctoral School: Prof. Lajos Bogár MD, PhD, Dsc.

Head of PhD Program: Prof. Attila Miseta MD, PhD, Dsc.

Mentor:

Tamás Nagy MD, PhD, Department of Laboratory Medicine



University of Pécs, Medical School

PÉCS

2024

SUMMARY

Diabetes and Alzheimer's disease (AD) affect millions of people worldwide separately, and a strong link has been found between the two conditions, both epidemiologically and biochemically. Insulin and insulin-like growth factor production and resistance to insulin receptors have been shown to decrease in association with glucose transporters (GLUT1 and GLUT3), and FDG-PET CT scans suggest that glucose metabolism in the central nervous system is lower compared to healthy individuals. Several factors are involved in the development of AD and are closely interrelated. O-Glycosylation is a reversible protein post-translational modification on the serine or threonine side chains of proteins, which has a broad regulatory role and is likely to be a common element in the pathogenesis of AD and diabetes.

My thesis consists of two parts, which are thematically related. In order to better understand the putative metabolic background of AD, a series of experiments were performed in a neuroblastoma (SH-SY5Y) cell line for 24 h in a hypoglycaemic environment. Six different glucose concentrations were adjusted extracellularly (EC): 0.5; 0.8; 1.3; 1.8; 3 and 5 mM. After the incubation period, in addition to glucose and lactate levels, oxygen consumption (OCR) and medium acidification (ECAR) were determined, as well as ATP and intracellular glucose levels. We monitored cell morphology, viability and cell division rate, as well as the rate of O-glycosylation. Our results indicate that below a glucose concentration of 1.8 mM, the metabolism of SH-SY5Y cells is altered: the decrease in the amount of glucose available for EC is compensated by a change in the ratio of glycolysis/oxidative phosphorylation; ECAR decreases, thus the oxygen consumption rate (OCR) to oxygen consumption rate (OCR/ECAR) increases exponentially. Their division rate gradually decreases, but their viability starts to decline at very low glucose concentrations; 0.5 mM. Previously used cellular models using total glucose deprivation induced an acute stress response in cells with an increase in O-glycosylation, whereas in our present model we were able to induce a decrease in this during a gradual hypoglycaemia. We believe that moderate glucose deprivation provides a better model for the metabolic alterations in AD and may explain the reduced O-glycosylation in pathological tissues and the resulting hyperphosphorylated tau proteins and amyloid-beta (A β) accumulation.

In the second part of the thesis, I will present the relationship of haemoglobin A1c (HbA1c), currently the most commonly used in the diagnosis and treatment of diabetes, with fasting plasma glucose. This has been characterised mainly by linear equations, but after retrospective analysis of nearly 15 years of data stored in our laboratory's system (GLIMS), we believe that

a non-linear modelling based on Michaelis-Menten (MM) kinetics is more appropriate and accurate, especially for the extreme values. By using this, an individual-specific Michaelis index can be determined, while changes in HbA1c can be estimated even on a daily basis, thus helping to design an individualized treatment plan for diabetes.

INTRODUCTION

The brain's main source of energy is glucose. It has a high demand for sugar relative to its relative mass, but it can adapt to hypoglycaemia within certain limits, as neurons can use lactate and ketone bodies as alternative nutrients. This requires the close involvement of astrocytes. Hypoglycaemia causes the release of glutamate from neurons, which is taken up by astrocytes via specific glutamate transporters together with Na⁺ ions. Glutamate is converted to glutamine by an ATP-dependent reaction that stimulates glucose uptake. The increase in the intracellular Na⁺ gradient activates the Na⁺-K⁺ ATPase, which triggers glycolysis. Lactate production is increased, released into the EC space and then used by neurons as a source of energy for ATP production. In brain tissue, the glucose concentration is 1-2 mM. In the short term, intracerebral glycogen may also serve as a nutrient in hypoglycaemia. The metabolites from lactate are used in the Krebs cycle, while glucose can also be used in the pentose-phosphate pathway. Ketone bodies pass through the blood-brain barrier by passive transport, diffusion or via the monocarboxylate transporter 1 protein. In addition, aquaporin channels have also been discovered to play a role in the transport of β -hydroxybutyrate, which eventually enters the citric acid cycle in the mitochondria of cells as acetyl-CoA, providing additional energy to the cell. 88% of all ATP production takes place under aerobic conditions, with glycolysis producing 2 ATP and oxidative phosphorylation producing 28 ATP from one glucose, but can also be based on glycogen, fat or protein. In contrast, under anaerobic conditions, 2 ATP and 2 lactate molecules are produced per molecule of glucose. In this case the body can still use glycogen, but not fat or protein. So aerobic energy production is more efficient, but a hundred times slower than in anaerobic conditions. The microcellular environment determines which predominates. If ATP synthesis is impaired, this ultimately leads to impaired excitatory transmission, involving the decline in cognitive function and memory that is widely known in dementia. Mitochondrial dysfunction is one of the factors involved in the development of AD. In addition, the reactive oxygen free radicals generated lead to damage to lipids, proteins and nucleic acids, resulting in neuronal degeneration. The substrates of O-Glycosylation are derived from the hexosamine biosynthesis pathway, in which only 2-5% of total glucose enters, but are essential for post-translational modifications of certain proteins responsible for cell survival,

metabolism, signal transduction and modification of protein properties. It has also been shown to attenuate Ca^{2+} oversaturation and reactive oxygen free radical formation, thereby reducing mitochondrial permeability.

Neurofibrillary tangles and amyloid plaques are typical in AD. Tau phosphoprotein is normally present in soluble form, but upon hyperphosphorylation it forms insoluble bundles and deposits, impairing cytoplasmic function and axonal transport. In addition, accumulated tau may increase mitochondrial membrane potential, thereby reducing mitophagy and leading to an increase in the number of abnormal mitochondria, thus affecting the progression of AD. Phosphorylation and O-glycosylation are known to be reciprocally related. In animal models, it has been shown that hyperphosphorylation of pathogenic tau proteins is inhibited by increasing O-glycosylation. In addition, O-glycosylation levels in hippocampal cells are decreased in a time-dependent manner during starvation and increased during feeding in a mouse model. It is important to note that the difficulty of animal models in this case is that significant reductions in blood and brain glucose levels may be counteracted by gluconeogenesis. Paradoxically, hypoglycaemia has been shown to enhance O-glycosylation in a number of in vitro experiments, presumably acting as an acute stress response on neurons and possibly beneficial for cell survival. In Alzheimer's patients, this increase is not seen in chronic hypoglycaemia. In our opinion, previous experiments have not taken into account that neurons may adapt to lower glucose concentrations and the gradualness of this adaptation. Hypoglycaemia was achieved by blocking glycolysis or by complete deprivation of glucose, thereby increasing the level of O-glycosylation. Since this post-translational protein modification plays a key role in the pathogenesis of many diseases, it could be a potential therapeutic target and is therefore of increasing interest.

The close link between AD and type II diabetes is confirmed by both epidemiological studies and biochemical processes. The name type III diabetes was first used in 2005 when a post-mortem examination of AD patients revealed a disruption of insulin signalling in brain tissue, thus identifying it as a neuroendocrine disease. It was later confirmed that the risk factors for both diseases overlap to a large extent, and that insulin administration contributes to improved cognitive function. Insulin is also produced by brain tissue itself, can cross the blood-brain barrier and plays an important role in memory functions. Insulin resistance, a reduction in the number of GLUT1-3 receptors, in addition to vascular hypoperfusion, is also responsible for the development of AD.

In diabetes, the insulin signal is impaired and glucose does not enter the cell, starving most of the tissue cells. In many cases of high blood glucose, the glycated haemoglobin fraction in red

blood cells is elevated, the most commonly measured form being haemoglobin A1c (HbA1c). Glucose is transported into red blood cells by the insulin-independent glucose transporter GLUT1 and reacts with the N-terminal protein in the beta chain of haemoglobin A in a non-enzymatic process. HbA1c is formed throughout the lifetime of the red blood cell and is typically released only at the end of its life. It can therefore be stated that by measuring HbA1c, the average glucose concentration over the last 2-3 months can be monitored. Its level is influenced by gender, race, diet, certain medical conditions such as anaemia or kidney disease. Its reference value is expressed as a percentage, mg/dl or mmol/mol. The normal range is below 5.7%, up to 6.4% is prediabetes, while above 6.5% a diagnosis of diabetes can be made. The average glucose level can be determined on the basis of repeated measurements or continuous glucose monitors taken several times a day, which so far have been used to infer HbA1c levels mainly by calculations based on linear equations and vice versa. However, the measured and calculated values often differed; this has been termed the haemoglobin glycation index (HGI). Its significance lies in the fact that both over- and underestimated HbA1c do not lead to appropriate therapy. When the observed HbA1c is higher than the estimated one, patients with a positive HGI are more likely to suffer from complications due to inadequate therapy, while patients with a negative HGI also have a poor prognosis. The value and accuracy of HGI therefore depends on the HbA1c and AG values, i.e. the accuracy of the model used. Considering the complexity of HbA1c formation and the slow, gradual nature of the process, as well as the variable plasma glucose concentrations, current linear models are not perfect. Membrane transport of glucose is known to follow MM kinetics and may therefore be mainly responsible for the evolution of the glucose - HbA1c curve.

AIMS

The timelessness of the MM enzyme kinetics model is still evident today. Given that diabetes and Alzheimer's disease (AD) are endemic and closely related, our aim was to shed light on the links that are already useful both in basic research and in practice.

In the first part of this thesis, we investigated the hypoglycaemia tolerance of neuroblastoma cell lines using six different glucose concentrations of media in which SH SY5Y cells were incubated for 24 hours. Our precise objectives were:

- *Investigation of changes in cellular metabolism during adaptation to a prolonged hypoglycaemic environment.*

- *Monitoring the energy balance of cells.*
- *Monitoring morphology, viability and proliferation rate.*
- *Mapping the dynamics of O-Glycosylation, defining a critical glucose concentration where cells reach their maximum adaptability.*

In the second part of the thesis, we wanted to investigate the relationship between plasma glucose and HbA1c, because we hypothesised that using a non-linear model rather than the linear modeling used so far would provide more accurate results. In the second part of the thesis, we wanted to investigate the relationship between plasma glucose and HbA1c because we hypothesised that using a non-linear model rather than linear modelling would provide more accurate results. Thus, our objectives were:

- *Evidence for HbA1c formation based on Michaelis-Menten kinetics by analysis of clinical laboratory data.*
- *To refine the blood glucose and HbA1c conversion equation and improve the estimation of protein damage due to diabetes.*

MATERIALS AND METHODS

1. Cell culturing, method of treatment

SH-SY5Y neuroblastoma cell line (ATCC CRL-2266 human neuroblastoma) was used. It was cultured in EMEM-Ham's F12 1:1 medium, digested with 10% fetal bovine serum, antibiotic and 1% essential amino acids, and then equal amounts of cells were divided into 6 different flasks of 25 cm² each or into 6-, 24-, 96-well cell culture plates. When 65% confluence was reached, and the appropriate time point was determined by the Lineweaver-Burk diagram based on the measured glucose depletion, the cells were incubated for 24 h in RPMI 1640 medium supplemented with 10% fetal bovine serum, 1% essential amino acid and 5 mM glucose. At the end of this time, the medium was changed to RPMI 1640 at 0.5-; 0.8-; 1.3-; 1.8-; 3- or 5 mM glucose concentrations for 24 h. (Incubation times varied in previous series of experiments, see full dissertation.)

2. Cell morphology and proliferation

To monitor cell morphology and proliferation rate, a phase-contrast microscope (JuLi Stage Real Time Cell History Recorder (NanoEnTek) with live image technology) with 10x objective magnification was used during 24 h incubation in media with different glucose concentrations

(0.5; 0.8; 1.3; 1.8; 3 or 5 mM). Cells were incubated in a 24-well cell culture plate. The instrument took photographs of the preset areas every 30 min for 24 h. The associated software automatically calculated and quantified the proliferation rate based on the background and cell density, which was used to generate a graph of the estimated cell division rate using Excel.

3. Glucose-, lactate- and ATP measurement

EC glucose and lactate levels were measured from the medium before and after treatment using a Cobas Integra® 400 plus analyzer (Roche, Germany) according to the manufacturer's instructions. Intracellular glucose and ATP levels were measured using a minimally modified protocol introduced by Csepregi. An average of 400 000 cells per well was plated on a 96-well plate the day before treatment. A multimode plate reader (Perkin Elmer EnSpire Multimode reader, Waltham, MA, USA) was used for detection.

Theoretically, 2 lactates are produced from 1 molecule of glucose, thus the lactate conversion rate can be calculated using the following equation:

$$\text{Lactate conversion \%} = \frac{\text{average lactate production}}{\text{average glucose depletion} \times 2} \times 100$$

Total theoretical maximum ATP production can be calculated based on the concentration of glucose and lactate. In theory, 2 ATP is produced in glycolysis and 28 ATP in oxidative phosphorylation (OxPhos). Therefore, ATP production can be calculated using the equation below, in which:

$$\text{ATP from glycolysis} = \frac{\text{lactate production}}{2} \times 2$$

$$\text{ATP from OxPhos} = \left(\text{glucose depletion} - \frac{\text{lactate production}}{2} \right) \times 28$$

$$\text{Total ATP} = \text{ATP from glycolysis} + \text{ATP from OxPhos}$$

It was assumed in glycolysis, only 2 ATP emanate, while in the OxPhos, 28 ATP were produced, in which glucose was only used for glycolysis. Based on glucose consumption, we developed the Lineweaver-Burk plot to calculate K_m and V_{max} , of which, were 3.68 and 2.4552. The theoretically calculated glucose uptake rate was compared with the measured rate by using Michaelis-Menten Kinetics:

$$V_{act} = (V_{max} \times S) / (K_m + S)$$

(V_{act} : actual velocity, V_{max} : maximal rate of the reaction, S: substrate concentration, K_m : substrate concentration once the reaction rate is half of V_{max})

4. Cell viability

The 3-(4,5-dimethylthiazol-2-yl)-2,5-diphenyl-2H-tetrazolium bromide (MTT) assay (Millipore Sigma, Item No. M2128) was used for apoptosis assay. After treatment, the cells were washed three times with a single PBS solution and 150 μ l of MTT solution was pipetted per well onto a 96-well cell culture plate. After four hours incubation, the resulting formazan crystals were dissolved in 100 μ l dimethyl sulfoxide (DMSO) solution. Absorbance values were measured at 450 nm using a multimode plate reader (Perkin Elmer EnSpire Multimode reader, Waltham, MA, USA).

5. Oxygen consumption rate and extracellular acidification measurement

Cells were incubated for 24 h in the above described glucose medium in 6-well plates and oxygen consumption rate (OCR) and EC acidification rate (ECAR) were detected during the last 3 h of treatment using an Agilent Seahorse Extracellular Flux (XF HS Mini Analyzer) Analyzer (Agilent Technologies, Santa Clara, CA, USA). The results were normalized to the respective protein concentration determined using DCTM Protein Assay Kit II (Bio-Rad, Item No. 5000112).

6. Monitoring the dynamics of O-Glycosylation, Western blot analysis

The pre-treated cells were harvested and stored at -80 °C until use after washing three times in PBS. After thawing, the cells were digested in modified RIPA buffer and, after centrifugation at 3500 rpm for 10 min at 4 °C, the protein content was determined from the supernatant using DCTM Protein Assay Kit II (Bio-Rad, Item No. 5000112). Samples for single run were adjusted to the lowest measured concentration. For conventional Western blotting, lysates were boiled with Laemmli buffer for 5 min, whereas for the capillary-based automated Western blotting system coherent with the conventional method, a modified buffer was used. Samples were run on an 8% SDS-PAGE gel and blotted onto PVDF membrane. RL2 antibody specific for O-glycosylation was used as antibody and anti-actin IgG antibody as internal control. Incubation was overnight at 4 °C. The membranes were then incubated with the corresponding horseradish root peroxidase-conjugated secondary antibodies for 2 hours. After washing steps, chemiluminescent detection was performed with Syngene G:boxx, SuperSignal™ West

Femto Maximum Sensitivity (Thermo Fisher Scientific) substrate. After the 24 h protocol, the run was performed with WesTM (Bio-Techne, ProteinSimple, Article No. 004-600), according to the manufacturer's instructions, using a 12-230 kDa separation module (ProteinSimple, Article No. SM-W004) and RL2 and GAPDH primary antibody, in addition to the factory Anti-Mouse Detection Module (ProteinSimple, Article No. DM-002). The tool performed the priming steps automatically. The resulting images were analysed using ImageJ software.

7. Study population

We retrospectively collected the measurement results from 18 April 2007 to 6 April 2021 from our laboratory information system (GLIMS). The inclusion criterion was that an order had to include haemoglobin, plasma glucose and HbA1c values simultaneously. This was met by a total of 175,437 orders containing information on 46,646 subjects.

8. Blood sampling

Tubes containing potassium ethylenediaminetetraacetate (K-EDTA) were used to collect peripheral venous blood samples for CBC (complete blood count) measurement, including haemoglobin and HbA1c analysis. Tubes containing sodium fluoride (NaF) were used to measure plasma glucose. CBC and haemoglobin were measured using multi-parameter automated haematology analysers Cell-Dyn 3700 system (Abbott Diagnostics, IL, USA), ADVIA 120 and 2120 (Siemens Healthcare GmbH, Erlangen, Germany) and SYSMEX XN-series (Sysmex Corporation, Kobe, Japan). Plasma glucose was detected on various Cobas instruments: the Integra 400Plus, Cobas C502 and Cobas C702 (Roche Diagnostics, GmbH, Mannheim, Germany) use the hexokinase method. HbA1c was first measured on a Modular P800 analyzer (Roche Diagnostics, GmbH, Mannheim, Germany) using an immunoassay, and then on an Arkray ADAMS A1c (Arkray Inc, MN, USA) ion-exchange high-performance liquid chromatograph (HPLC) analyzer, and, more recently, on a Tosoh G11 (Tosoh Bioscience, Tokyo, Japan) ion-exchange HPLC analyser (interassay variability 31 mmol/mol for 0.6% HbA1c, 84 mmol/mol for 0.5% HbA1c).

9. The kinetic model

The formation of HbA1c in red blood cells is determined by three processes: glucose entry into the cells, non-enzymatic glycation of the N-terminal valine of the beta chain, and red blood cell elimination. Of these, glucose membrane transport is the only one regulated by MM kinetics.

Non-enzymatic glycation follows pseudorapid kinetics, whereas red blood cell elimination follows a constant rate. Thus, the shape of the plasma glucose - HbA1c curve can be modelled by the MM equation, while non-enzymatic glycation and elimination can shift the curve mostly laterally. The model can be described by the following equation:

$$\text{HbA1c} = \frac{V_{\max} \times \text{pGlc}}{K_m + \text{pGlc}}$$

where pGlc is plasma glucose and V_{\max} is the maximum rate of HgbA1c, and was determined for the study population using the Lineweaver-Burk diagram. When V_{\max} is set to a fixed value and plasma glucose and HbA1c levels are measured simultaneously, the Michaelis constant (K_m) can be calculated. Inter- or intraindividual differences in the kinetics of HbA1c production are characterized by K_m . For comparison, we used the equation reported by ADAG for linear prediction of HbA1c:

$$\text{HbA1c (mmol/mol)} = \frac{\text{pGlc (mM)} - 0,8317}{0,14545}$$

Here pGlc is the average of plasma glucose levels over three months. Due to the retrospective nature of our study, we have replaced the average glucose with the actual plasma glucose levels. The general practice in the study population is to sample fasting after 10-12 h of fasting (except for patients on insulin therapy). The equation originally reported by ADAG does not take into account historical data, unlike the MM equation, so HGI values were calculated by subtracting measured HbA1c from the ADAG-predicted HbA1c. The current ADAG prediction was then corrected by the average of the previous HGI. When HbA1c was estimated using the MM equation, the average K_m value from the previous measurement was substituted into the current calculation.

10. Data analysis

For the cellular model, we used the SPSS20 program to analyze the data, and the results were presented as means and \pm standard deviations (SD). Comparisons were performed using one-way ANOVA, and in cases of significant differences ($p < 0.05$), Bonferroni or Dunnett T3 post hoc tests were applied. For the nonlinear kinetic model, we conducted correlation, regression, and ROC curve analyses using the SPSS20 software. When comparing individual ROC curves,

we used the MedCalc Statistical Software to perform the DeLong test. The results are presented as means and \pm SD values.

RESULTS

Investigation of the effect of hypoglycemia on a cellular model

1. Adaptation to the Michaelis-Menten glucose consumption kinetics

Our aim was to establish a relatively long-term experimental series that allows for adaptation to a hypoglycemic environment, thereby enabling the observation of responses induced by slow progression, similar to those seen in AD. Considering the duplication time of SH-SY5Y cells, we determined this time interval to be 24 hours. Initially, we set six glucose concentrations in the medium, which were subsequently controlled. After the 24-hour period, we remeasured glucose and lactate levels, from which the rate of glucose consumption and lactate production could be calculated. We found that glucose consumption was significantly lower in cells cultured in medium supplemented with 0.5 and 0.8 mM glucose compared to those treated with 5 mM glucose (0.29; 0.44 vs. 1.29 mM). Furthermore, glucose depletion, as a function of extracellular glucose concentration, followed a non-linear relationship. Since glucose transporters and all glycolytic steps follow Michaelis-Menten kinetics, we plotted our data on a Lineweaver-Burk plot (*Figure 1*).

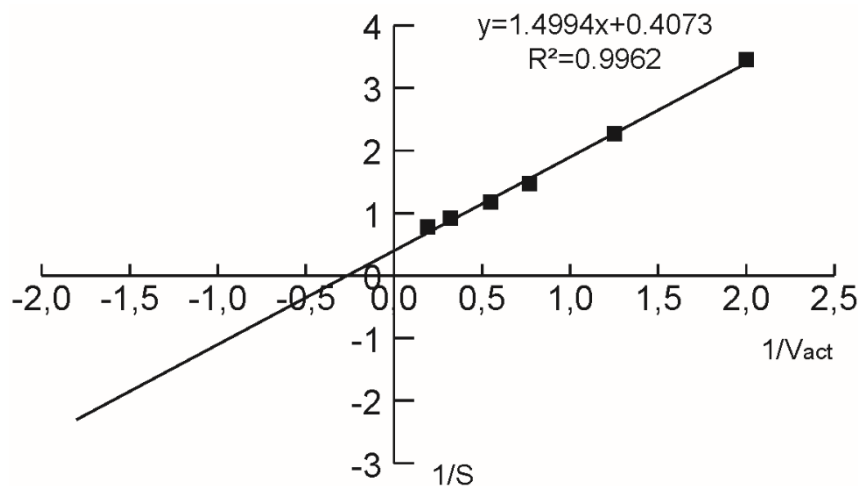


Figure 1: Lineweaver-Burk plot based on glucose consumption. Following Michaelis-Menten kinetics, V_{max} and K_m can be calculated.

Our experimental results closely aligned with the MM kinetic curve. The average deviation from the curve was 0.65% ($\pm 5.91\%$). We determined that under our experimental conditions, the K_m value was 3.68 mM (95% CI, 3.089 – 4.554 mM), and the V_{max} value was 2.4552 mM (95% CI, 2.0755 – 3.005 mM), which is characteristic of the SH-SY5Y cell line. According to MM kinetics, glucose consumption rapidly decreases at low EC glucose levels. Under normoglycemic conditions, SH-SY5Y cells convert glucose to lactate in an almost stoichiometric ratio ($\sim 70\text{-}80\%$). We found that this ratio begins to decrease below ~ 1.8 mM EC glucose concentration, while above this threshold, it remains relatively stable. Specifically, the lactate conversion ratios were 73.8% ($\pm 17.4\%$), 70.3% ($\pm 13.7\%$), and 42.35% ($\pm 18\%$) in cells incubated in medium containing 5 mM, 1.8 mM, and 0.5 mM glucose, respectively. We also assessed the metabolic contribution of glycolysis and oxidative phosphorylation by measuring the Oxygen Consumption Rate (OCR) and the EC Acidification Rate (ECAR). Similar to the lactate conversion ratios, the OCR/ECAR ratio remained unchanged between 5 mM and 1.8 mM but gradually increased below 1.8 mM EC glucose levels. In cells treated with 0.5 mM glucose, the OCR/ECAR ratio was significantly elevated, being three times higher compared to cells treated with 5 mM glucose (**Figure 2**). Thus, glycolysis was reduced to a fraction as the EC glucose concentration decreased.

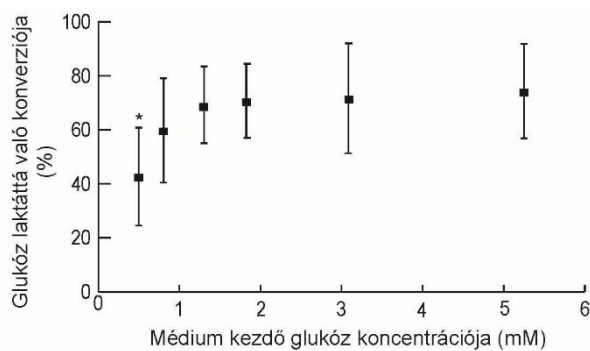
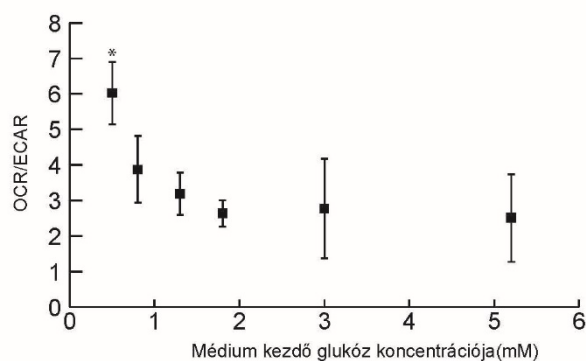


Figure 2:

Top: Glucose conversion to lactate after 24 hours of incubation. $n=7$

Bottom: Normalized OCR/ECAR ratios. Normalization was performed based on the protein concentration measured per well at the end of the experiment.



* $p < 0.05$ compared to the control 5 mM glucose concentration, using one-way ANOVA and Bonferroni post hoc test. $n=3$

2. Intracellular glucose measurement

The intracellular (IC) glucose level indicates the net balance between glucose uptake and the sum of IC glucose-utilizing processes. According to our results, there was no significant difference between the EC glucose conditions—meaning that the cells maintained their IC glucose levels consistently. There appeared to be a baseline IC glucose level of around $\sim 10 \mu\text{M}$, which did not drop below this threshold in any case, while an "extra" amount of EC glucose ($\sim 3 \text{ mM}$ and above) increased the IC glucose level as well.

3. ATP levels detections

Using the glucose consumption and lactate production data, we calculated the maximum attainable ATP levels, assuming that both glycolysis and oxidative phosphorylation operate at their theoretical maximum efficiency (**Figure 3A**). We found that the cells have significant reserves to maintain ATP levels by increasing the oxidative phosphorylation rate. Thus, theoretically, a cell exposed to EC glucose levels below 1.8 mM can significantly boost its ATP levels by utilizing lactate and increasing oxidative phosphorylation. To test this theory, we measured the actual ATP levels in the cells (**Figure 3B**). Surprisingly, the metabolic adaptation not only mitigated the impact of depleting energy sources, but ATP levels remained constant, with no significant differences observed in any case. This suggests that other adaptive mechanisms may be present beyond the OCR/ECAR ratio.

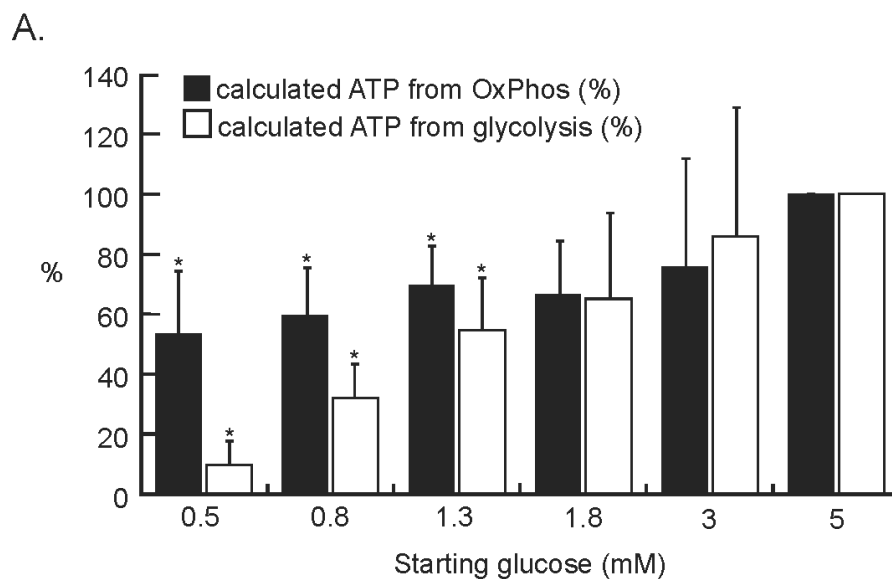


Figure 3A: Ratios of theoretical ATP levels calculated from OxPhos and glycolysis. $*p < 0.05$ compared to the control 5 mM glucose concentration, using one-way ANOVA and Dunnett T3 post hoc test. $n=5$

B.

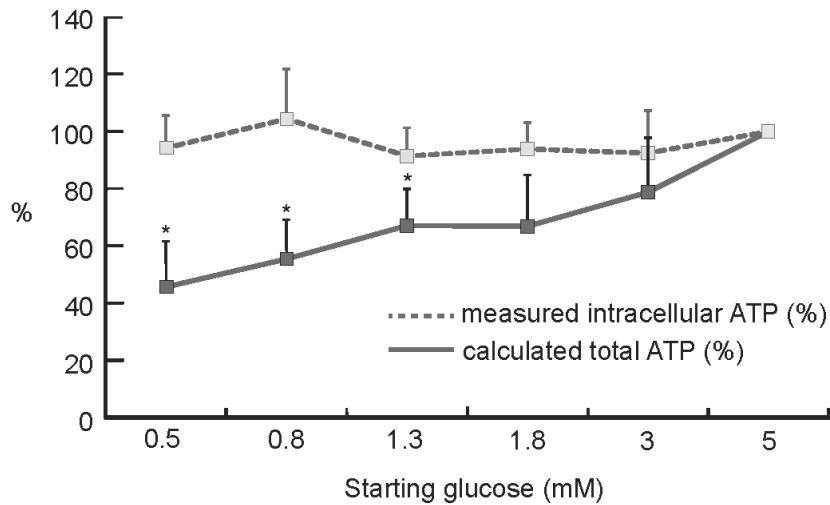


Figure 3B: Ratios of measured to calculated total ATP levels.

* $p < 0.05$ compared to the control 5 mM glucose concentration, using one-way ANOVA and Dunnett T3 post hoc test. $n = 5$

4. Investigation of cell viability

Cell viability was assessed using the MTT assay. Significant differences were observed only in cells cultured in medium containing 0.5 mM and 3 mM or 5 mM glucose, while no changes were detected in the other conditions. The average decrease was 17.8% ($\pm 9.5\%$) in the 0.5 mM glucose condition.

5. Cell proliferation and morphology

In contrast to primary neural tissue, SH-SY5Y neuroblastoma cells exhibit mitotic activity that can be influenced by glucose availability. Therefore, we assessed the cell division rate using a JuLi microscope. After 24 hours, the estimated division rate of cells treated with 0.5 mM and 0.8 mM glucose was significantly slower compared to cells incubated in medium with 5 mM glucose ($p = 0.007$ and $p = 0.027$, respectively). Direct microscopic observation also clearly demonstrated slower mitotic activity of cells under hypoglycemic conditions, although no morphological changes were found between different treatments, although the latter may not be considered entirely objective.

6. Investigation of O-Glycosylation

We validated the O-GlcNAc levels using Western blots (**Figure 5**). We selected five regions of interest (ROIs 1-5) from the proteins marked by the RL2 antibody, which are in the molecular weight range of approximately ~100 – 230 kDa, to analyze the effects of different hypoglycemic conditions (0.5 – 3 mM) within a 24-hour period compared to normoglycemic conditions (5 mM) (**Figure 6**). The O-GlcNAc levels were significantly reduced in cells treated with 0.5 mM EC glucose in the ROI 3-5 regions ($65\% \pm 17.68$). In the ROI 4-5 regions, the O-GlcNAc levels were also significantly reduced in cells treated with 0.8 mM EC glucose (ROI 4, 0.5 mM: $47.34\% \pm 12.94$; 0.8 mM: $59.02\% \pm 9.28$; ROI 5, 0.5 mM: $55.23\% \pm 14.73$; and 0.8 mM: $63.1\% \pm 10.84$) compared to the control conditions.

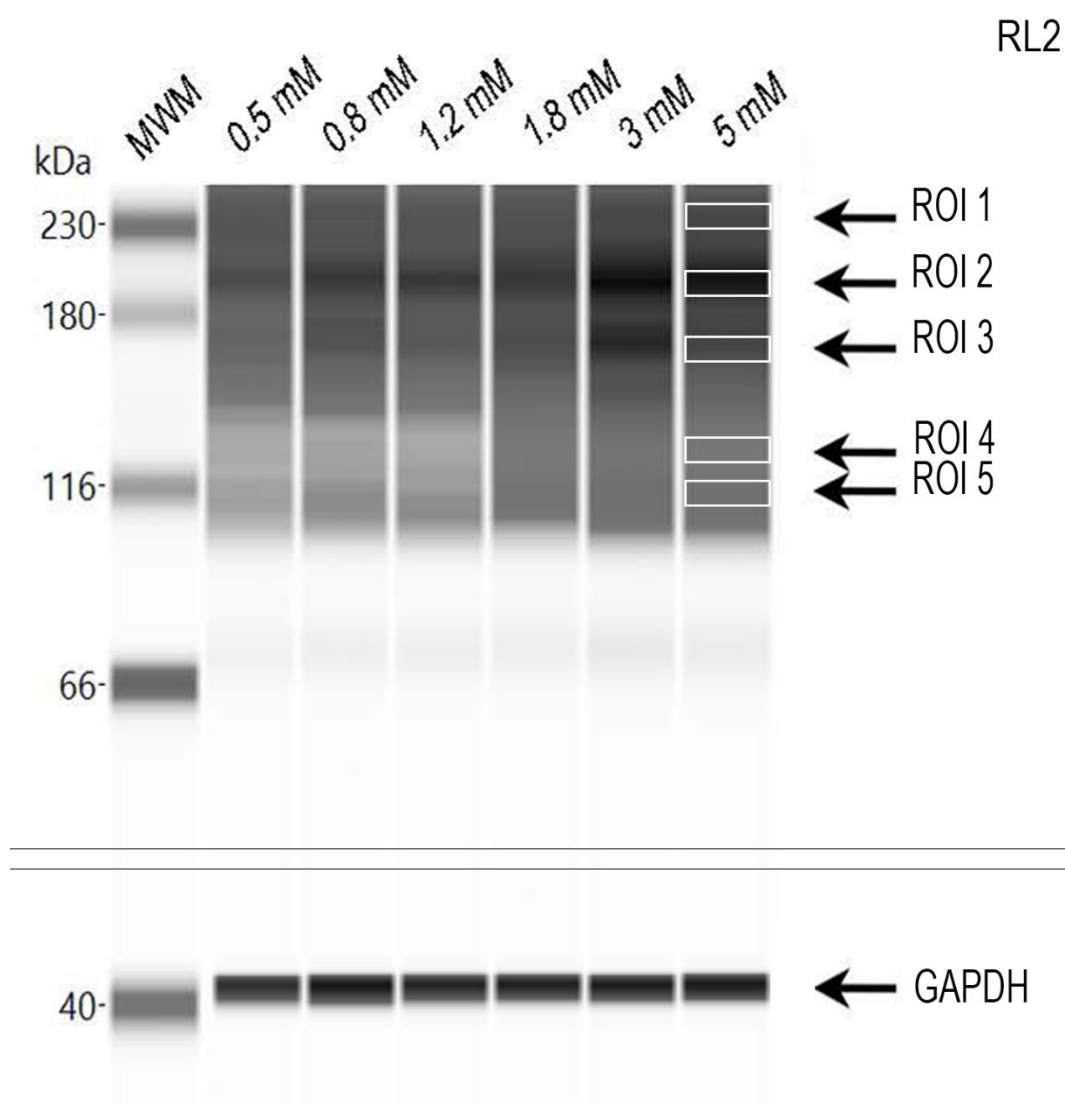


Figure 5: Representative Western blot of total SH-SY5Y cell lysate after 24 hours of treatment using the WesTM system. The extent of O-glycosylation was determined using the RL2 antibody, while GAPDH was also detected using its' antibody.

B.

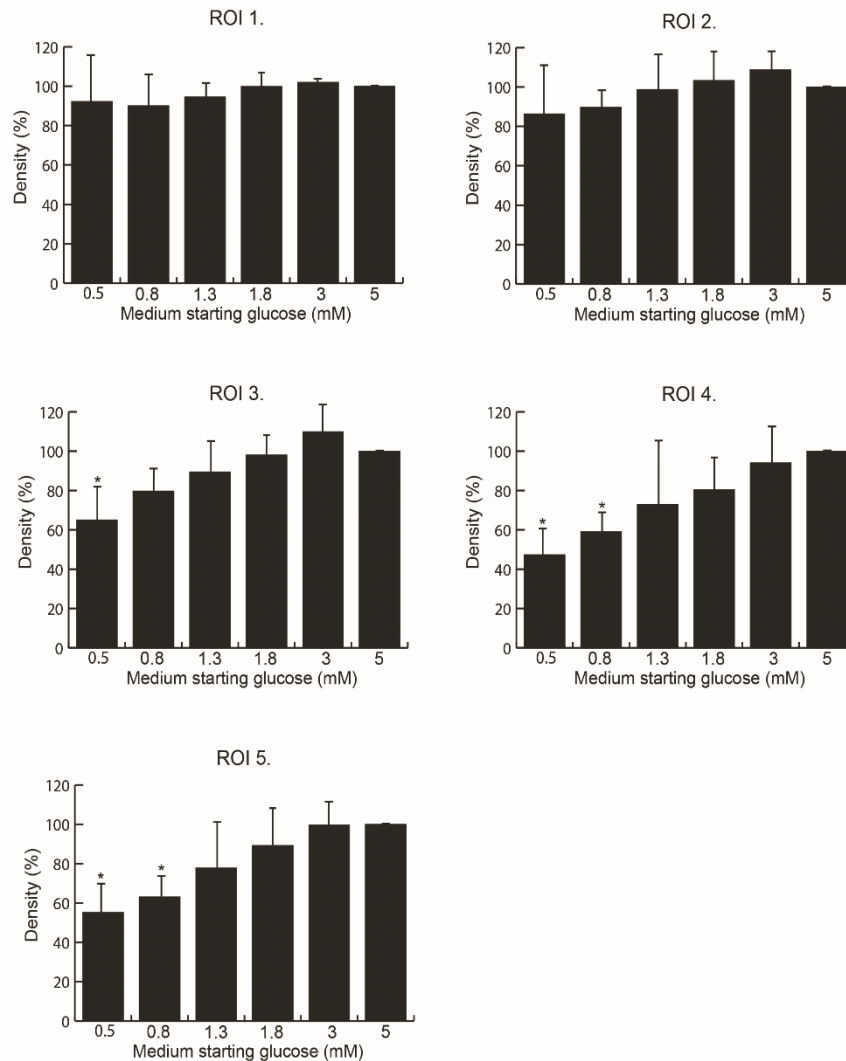


Figure 6:

*Analysis of Western blot regions. O-glycosylation was determined using the RL2 antibody, with GAPDH antibody serving as the control. The data were analyzed using ImageJ software. The figures show the density of the regions expressed as a percentage relative to the control (5 mM), along with SD values, as a function of the initial glucose concentrations in the medium. One-way ANOVA with Bonferroni post hoc test was used as the statistical test. * $p < 0.05$ $n = 6$*

Modeling the Relationship Between Plasma Glucose and HbA1c

We retrospectively analyzed 175,437 recorded laboratory results collected over 15 years, which included both plasma glucose and HbA1c data. The total number of patients was 46,646, with an average of 3.76 tests per person. The average time between visits was approximately 10 months. A total of 4,686 patients had 10 or more entries, with the average time between entries

being 6.2 months (as Hungarian health insurance covers up to 4 HbA1c tests per year). **Figure 7A** shows the distribution of measured plasma glucose and HbA1c results.

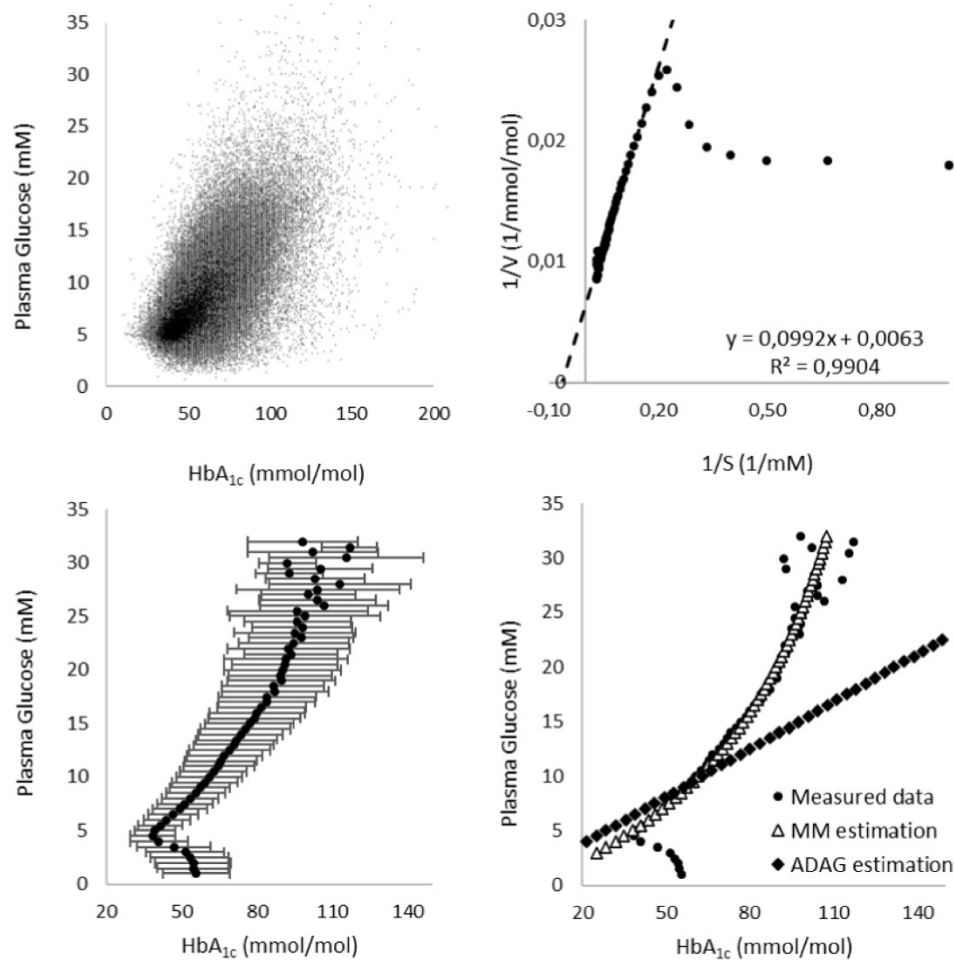


Figure 7: The relationship between HbA1c and simultaneously measured plasma glucose levels. (A) Raw data, showing 175,437 events. (B) Presentation of average (\pm SD) HbA1c values. Each data point represents a 0.5 mM plasma glucose concentration range. (C) Lineweaver-Burk plot of HbA1c kinetics. The reciprocal values of average HbA1c levels ($1/v$) are plotted against the reciprocal values of corresponding plasma glucose levels ($1/S$). (D) Prediction of average HbA1c values using the MM ($V_{max} = 158.7$ mmol/mol and $K_m = 15.7$ mM) and linear (ADAG) equations compared to the observed average HbA1c values.

We compared HbA1c results with the corresponding plasma glucose values, categorizing each by a 0.5 mM plasma glucose range. As shown in **Figure 7B**, the average HbA1c values appear to have a maximum limit. When plotting the average HbA1c and plasma glucose values on a Lineweaver-Burk plot (**Figure 7C**), the data displayed a linear pattern between glucose values of 5–32 mM, suggesting that HbA1c formation follows Michaelis-Menten (MM) kinetics. By interpolating the linear trendline, the V_{max} was determined to be 158.7 mmol/mol (95% CI, 112.5–269.5 mmol/mol), while the K_m was 15.7 mM (95% CI, 15.2–16.3 mM). Considering

this K_m value as the population average, we found that the HbA1c levels predicted by MM closely matched the observed average levels (**Figure 7D**).

We tested the prognostic potential of the MM equation at the individual level. Using the first five data pairs, we calculated the average K_m parameter. Then, we predicted the expected HbA1c levels based on the glucose concentration at the 6th visit, using either the MM equation or the ADAG equation. The MM equation demonstrated better prognostic power; however, the predictive accuracy of both equations declined over time, indicating that an individual's K_m value may change continuously. This can be offset by updating the K_m value at each visit. To further confirm the relative stability of K_m , we plotted the K_m values (average of the first 5 visits) against the average HbA1c value from the first 5 visits, the 6th visit, and the average of the second 5 visits. The data points were color-coded according to the corresponding average plasma glucose levels (**Figure 8**). As expected, patients with higher plasma glucose concentrations generally had higher HbA1c levels. Interestingly, K_m appears to have a gradual inverse relationship with HbA1c. We assessed the predictive potential of the MM equation using individual K_m values through ROC analysis (**Figure 9A**), with a positive classification cutoff value of 37.7 mmol/mol. In this comparison, the MM model was significantly different ($p < 0.0001$) and outperformed ADAG.

The prognostic value of the MM model truly stands out when patients experience significant changes in plasma glucose levels over time. **Figure 9B** shows the average K_m value from the first 5 measurements of patients in relation to the average HbA1c levels from the second 5 measurements, specifically for those whose glucose levels were above 7 mM during visits 1–5, but then averaged below 7 mM in subsequent visits. Despite the significant decrease in glucose levels, the K_m value continued to show a negative correlation with the measured HbA1c levels. When these K_m values (average of visits 1–5) were combined with the actual glucose concentrations (visits 6–10) in the MM equation to calculate the estimated average HbA1c for visits 6–10, a significant correlation was found with the measured HbA1c levels ($r^2 = 0.52$) (**Figure 9C**). Using the same selection criteria, the ADAG prediction, corrected by the average HGI (from visits 1–5), had a lower coefficient of determination ($r^2 = 0.312$). (**Figure 9. D**)

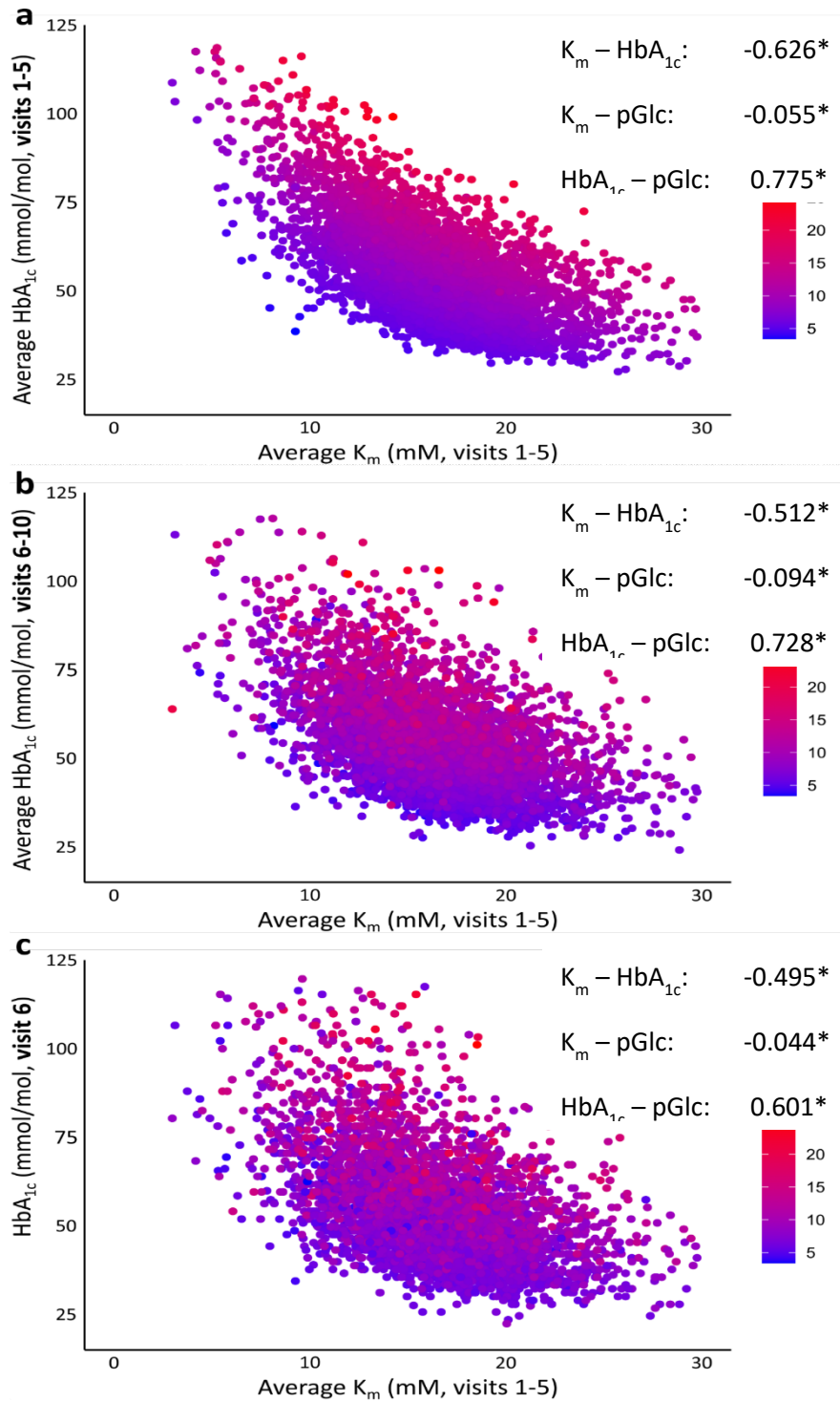


Figure 8: Correlation between HbA1C, K_m , and plasma glucose levels. $N = 4686$; individuals with at least 10 visits were selected. Data points are color-coded according to the plasma glucose (pGlc) level at visit 6. Spearman's rho correlation coefficients are indicated for each data pair, with significance denoted by asterisks. (A) Depicts the average HbA1C and K_m values from the first 5 visits. (B) Compares the average HbA1C values from the second 5 visits with the average K_m values from the first 5 visits. (C) Compares the HbA1C value at visit 6 with the average K_m values from the first 5 visits.

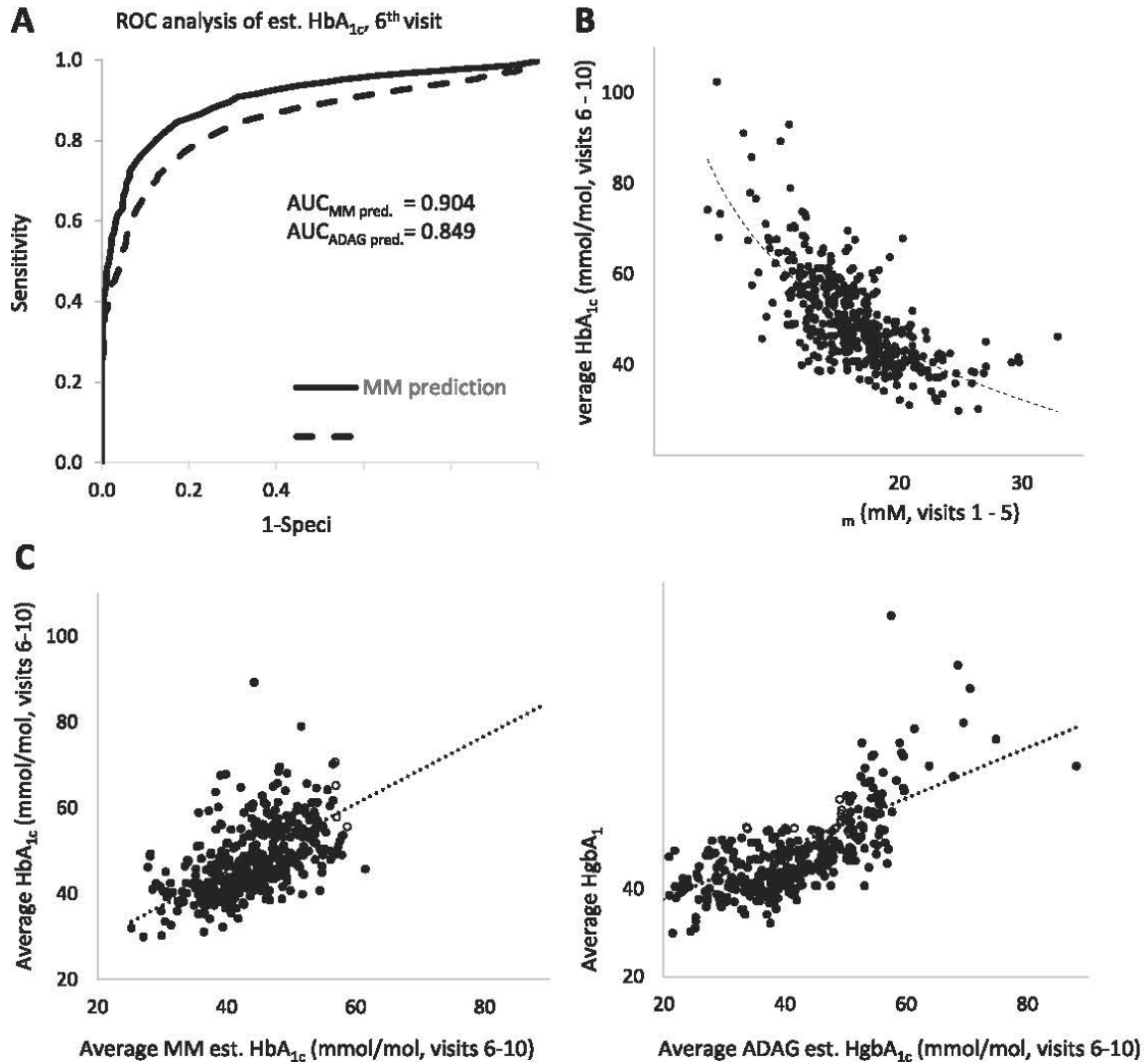


Figure 9: Predictive Power of MM and ADAG Estimates. (A) Predictive Receiver-Operating Curve (ROC) analysis based on consecutive records of 4,686 individuals. For the MM calculation, personalized K_m values were selected by averaging the K_m values from the first 5 visits. These K_m values and the measured plasma glucose levels at the 6th visit were substituted into the MM equation. For the ADAG calculation, the plasma glucose levels from the 6th visit were input into the linear equation, adjusted by the average HGI value from the first 5 visits. The dependent variable was the measured HbA1C level at the 6th visit. (B) Individuals were selected who had an average glucose level above 7 mM during the first 5 visits but below 7 mM during the second 5 visits ($N = 427$). K_m values were calculated using the HbA1C and plasma glucose levels measured during the first 5 visits and plotted against the average HbA1C levels measured during the second 5 visits. (C&D) In the same dataset as in point B, HbA1C levels predicted by MM and ADAG (corrected by HGI) calculations were compared with measured HbA1C levels (MM: $R^2 = 0.517$, $P < 0.001$, ADAG: $R^2 = 0.312$, $P < 0.001$, linear regression model).

DISCUSSION

AD and diabetes are considered widespread public health issues, making it our responsibility to precisely map out the pathways leading to their development, just as it is to implement effective therapies. By gaining a better understanding of the processes that lead to these diseases, we may not only explain them more effectively but also discover tools for their prevention.

In the first part of my thesis, we aimed to gather more precise knowledge about the metabolic behavior of neural-derived cells using the described cellular model, specifically in cases where the hypoglycemic environment develops slowly, gradually, and persists for a relatively long period. This approach could provide a foundation for a more accurate understanding of AD progression. There have already been studies in the literature addressing this area. The challenge with animal experimental models is that the body's compensatory mechanisms work against the disruption of brain glucose homeostasis. From this perspective, cellular models prove to be more advantageous when we seek to examine the underlying biochemical processes. Several cell groups have already been exposed to the effects of hyper- and hypoglycemia, including investigations into changes in O-glycosylation. However, the results have been contradictory; in cases of both hyper- and hypoglycemia, an increase in O-glycosylation was primarily observed. We believe this may have been due to the initiation of an acute stress response in the cells caused by rapid or complete glucose deprivation. In our current series of experiments, during the 24-hour incubation of SH-SY5Y cells, they responded to the gradually decreasing glucose concentration by restructuring their metabolism. During this adaptation, the ratio of oxidative phosphorylation to glycosylation changed; glycosylation decreased more significantly, which led to an increase in the OCR/ECAR ratio. We detected that the amount of ATP derived from glycolysis decreased more substantially than the ATP derived from oxidative phosphorylation, although their overall levels did not differ significantly. Given that fructose-6-phosphate, one of the substrates of the hexosamine pathway, also originates from glycolysis, its decrease may lead to a reduction in O-glycosylation as well. Additionally, our experimental results closely matched the Lineweaver-Burk plot based on glucose utilization ($R^2=0.9962$), following MM kinetics, allowing the calculation of V_{max} and K_m . These values are characteristic of the given cell line in the described experimental series. During the monitoring of proliferation, the cell division rate decreased, which corresponds to the findings in the literature, indicating that the decrease in mitotic activity can be explained by the depletion of available glucose. Neuroblastoma cells strive to adapt to unfavorable environmental conditions as much

as possible, attempting to maintain both their ATP levels and intracellular glucose levels at a constant level. However, a trend was observed: at glucose concentrations above 3 mM, higher values were obtained, indicating that the intracellular glucose level decreases below this threshold. Nevertheless, even at 0.5 mM, it does not drop below a minimal level (~10 μ M). In terms of viability, a significant decrease was detected in cells maintained in a medium with 0.5 mM glucose concentration. A limitation of this research is that the neuroblastoma cell line likely possesses a greater adaptive potential than primary neuronal cells, as the latter mainly obtain ATP through aerobic oxidative phosphorylation. When glucose availability decreases, neurons rely on the assistance of astrocytes, which can break down their glycogen stores, converting it first into glucose-1-phosphate by glycogen phosphorylase, then into glucose-6-phosphate by phosphoglucomutase. This is then oxidized into pyruvate during glycolysis, which lactate dehydrogenase (LDH) converts into lactate. Astrocytes do not express glucose-6-phosphatase, so they cannot deliver free glucose to neurons, but neurons can utilize lactate to meet their energy needs. Although both cell types contain lactate dehydrogenase, astrocytes primarily express the LDH5 isoform, while neurons express LDH1, which primarily converts lactate into pyruvate, further emphasizing the dominance of oxidative metabolism. The expression ratio of these enzyme isoforms also varies depending on the brain region. Lactate is exported from astrocytes via MCT-1 and taken up by neurons through MCT2. The transport of lactate is highly dependent on extracellular pH, which may explain why lactate uptake by the brain increases when its levels rise in the blood. E. Lezi and colleagues, including Swerdlow, treated SH SY5Y cells with high concentrations of lactate and found that cellular respiration increased, bioenergetic processes shifted towards aerobic pathways, and the rate of glycolysis decreased. This was accompanied by changes in insulin signaling and various proteins and post-translational modifications involved in these processes. In our research, we observed a similar metabolic shift; however, the lactate concentration was nowhere near as high as that used in the aforementioned treatment.

In the future, we plan to conduct this series of experiments on primary neuronal cells and astrocytes as well. Additionally, we aim to test the application of alternative nutrients, such as β -hydroxybutyrate.

In the study presented in the second part of this dissertation, we confirmed that HbA1c levels can be predicted with greater accuracy using MM kinetics compared to linear models. In this research, we retrospectively analyzed a large number of plasma glucose and HbA1c records from the past 15 years, collected from more than 46,000 individual patients, with approximately

10% having more than 10 consecutive measurements. The Michaelis constant, K_m , emerged from the model as a useful biomarker for assessing individual differences. K_m could be introduced as a new metabolic parameter, potentially surpassing the predictive value of previous markers, such as the hemoglobin glycation index, the glycation gap, or the glucose management indicator. The relative stability of K_m over time also ensures that the conversion of plasma glucose levels to HbA1c remains reliable over longer periods. HbA1c is formed throughout the lifespan of red blood cells and is eliminated from circulation as they are destroyed. The membrane transport of glucose is well-known to follow Michaelis-Menten (MM) kinetics, and this main process is responsible for the shape of the glucose-HbA1c curve. In our study, we found that the MM equation used to calculate HbA1c better represents the underlying mechanisms, more accurately describes the glucose-HbA1c relationship, and thus has superior predictive capability. Additionally, MM kinetics can be effectively utilized even with limited data—specifically, when only fasting glucose measurements are available. A limitation of our study is that our sample population consists predominantly of Hungarian, Caucasian individuals, and therefore, adjustments to V_{max} may be necessary for other racial groups. The effects of GLUT1 activity, as well as age, sex, race, and the ratio of fasting to postprandial glucose, must also be considered. It is important to note that rare hemoglobin variants can interfere with the analysis. HPLC analyzers separate labile glycated hemoglobin from stable HbA1c, but sudden changes in glycemic status can increase the amount of the labile fraction, potentially overlapping with the stable fraction. Variability in glycation and RBC elimination rates remains a problem. In summary, we believe that current linear models and calculations could be replaced by the MM equation. Existing web-based calculators and mobile applications could be easily updated, allowing patients and physicians to monitor therapy/diet progress between mandatory laboratory HbA1c checks. Introducing K_m as a quantitative parameter would also enable the differentiation of "poor responders," who have difficulty reducing HbA1c without risking hypoglycemia. For these patients, alternative therapeutic approaches should be considered. Standardized K_m , as a biomarker, could also aid in evaluating and better understanding the metabolic effects of comorbidities.

SUMMARY OF NEW RESULTS

1. Investigation of the effects of hypoglycemia on a cellular model

We aimed to study the effects of chronic hypoglycemia on the neuroblastoma (SH SY5Y) cell line. For this purpose, we incubated the cells in six different glucose concentration media for 24 hours. We found the following:

- *SH-SY5Y cells compensate for glucose deprivation by altering the glycolysis/oxidative phosphorylation ratio at glucose concentrations below 1.8 mM.*
- *ECAR decreases, resulting in an exponential increase in the ratio of oxygen consumption (OCR) to ECAR (OCR/ECAR), without a change in the total ATP level.*
- *Cell viability of neuroblastoma cells significantly decreases in media with 0.5 mM glucose concentration, while a slowdown in cell proliferation is already observed at glucose levels below 1.3 mM compared to the control (5 mM).*

In our model, gradually developing hypoglycemia led to a decrease in O-Glycosylation. We believe that moderate glucose deprivation may provide a better model for the metabolic alterations seen in Alzheimer's disease.

2. Modeling the relationship between plasma glucose and HbA1c

In our study, we retrospectively analyzed nearly 15 years of data containing HbA1c and plasma glucose values stored in our laboratory's information system.

- *After graphically representing the associated data pairs, we concluded that non-linear modeling based on Michaelis-Menten kinetics is more effective and accurate compared to the linear equations previously used, especially concerning extreme values.*
- *Applying the new calculations can reduce therapeutic uncertainty and enable more precise treatment using the individual-specific Michaelis index.*

PUBLICATIONS

Articles related to the thesis

Nagy Zsófia; Poór Viktor S; Fülöp Norbert; Chauhan Deepanjali ; Miseta Attila; Nagy Tamás: *Michaelis-Menten kinetic modeling of Hemoglobin A1c status facilitates personalized glycemetic control*. CLINICA CHIMICA ACTA (0009-8981 1873-3492): 548 Paper 117526. 8 p. (2023) IF: **5.0**

Zsófia Nagy; Rita Csepregi; Emese Kátai; Attila Miseta; Katalin Ördög; Róbert Halmosi; Tamás Nagy: *Metabolic shift may influence protein O-GlcNac modification in SH-SY5Y cells in a hypoglycemic AD model* – under publication

Articles not related to the thesis

Nagy Zsófia; Papp Ábel; Kristály Christopher; Horváth L. Levente; Béri Laura; Nagy Tamás; Vámos Zoltán: *Induktív keringésmegállás során felszabaduló neuronspecifikus enoláz és S100b neurobiomarker preanalitikai mérési hibalehetőségei*. Ideggyógyászati Szemle, Proceedings/ Clinical Neuroscience Proceedings szakfolyóirat, ISSN 2498- Megjelenés: (2023)

Papp Ábel; Kristály Christopher; Horváth L. Levente; Béri Laura; Kittka Bálint; Nagy Tamás; **Nagy Zsófia**; Vámos Zoltán: *Hemodinamikai instabilitás okozta S100b neurobiomarker szérumkoncentráció-változása*. Ideggyógyászati Szemle, Proceedings/ Clinical Neuroscience, Proceedings szakfolyóirat, ISSN 2498-6240 Megjelenés: (2023)

Kristály Christopher; Papp Ábel; Horváth L. Levente; Béri Laura; Kittka Bálint; Nagy Tamás; **Nagy Zsófia**; Vámos Zoltán: *Neuronspecifikus enoláz-szérumkoncentráció változása pacemakerrel indukált periarrest állapotban*. Ideggyógyászati Szemle, Proceedings/ Clinical Neuroscience Proceedings szakfolyóirat, ISSN 2498-6240 Megjelenés: (2023)

Karsai István; **Nagy Zsófia** ✉; Nagy Tamás; Kocsor Ferenc; Láng András; Kátai Emese; Miseta Attila; Fazekas Gábor; Kállai János: *Physical exercise induces mental flow related to catecholamine levels in noncompetitive, but not competitive conditions in men*. SCIENTIFIC REPORTS (2045-2322 2045-2322): 13 Paper 14238. 10 p. (2023) IF: **4.6**

Nagy Zsófia ✉; Karsai István; Nagy Tamás; Kátai Emese; Miseta Attila; Fazekas Gábor; Láng András; Kocsor Ferenc; Kállai János: *Reward Dependence-Moderated Noradrenergic and Hormonal Responses During Noncompetitive and Competitive Physical Activities*. FRONTIERS IN BEHAVIORAL NEUROSCIENCE (1662-5153): 16 Paper 763220. 11 p. (2022) IF: **3.0**

Nagy Tamás; Fisi Viktória; Frank Dorottya; Kátai Emese; **Nagy Zsófia**; Miseta Attila: *Hyperglycemia-Induced Aberrant Cell Proliferation; A Metabolic Challenge Mediated by Protein O-GlcNac Modification*. CELLS (2073-4409): 8 9 Paper 999. 29 p. (2019) IF: **4.366**

Nagy Zsófia; Kátai Emese; Miseta Attila; Nagy Tamás: *Stress Tolerance and Protein O-GlcNAc Regulation in Neuroblastoma Cells under Hypoglycemic Condition*. *Experimental Biology* 2019-04-06 [Orlando (FL), Amerikai Egyesült Államok] Megjelenés: (2019), poster

Darnai G; Szolcsányi T; Hegedüs G; Kincses P; Kállai J; Kovács M; Simon E; **Nagy Zs**; Janszky J: *Hearing Visuo-tactile Synchrony - Sound-Induced Proprioceptive Drift in the Invisible Hand Illusion*. *BRITISH JOURNAL OF PSYCHOLOGY* (0007-1269 2044-8295): 108 1 pp 91-106 (2017) IF: **2.507**

Impact factor of publications related to the thesis: 5.0

Cumulative impact factor: 19.473

ACKNOWLEDGEMENTS

I would like to express my sincere gratitude to my supervisor, Dr. Tamás Nagy, for his support and patience over the past years. I am grateful for his acceptance and his professional and personal support, as his valuable advice has proven beneficial both in my research and in teaching.

I also wish to thank Prof. Dr. Attila Miseta for believing in me from the very beginning and supporting every aspect of my ideas.

My thanks go to Dr. István Karsai for standing by me and supporting me from the early stages of my research work.

I am grateful to Dr. Ildikó Bock-Marquette for her assistance in my research, her valuable experience, her friendship, and her unwavering support from the outset in all areas.

I sincerely thank my colleagues Dr. Emese Kátai, Dr. Rita Jakabfi-Csepregi, Heléna Halász, Dr. Barbara Réger, István Német, and Dr. Zoltán Vámos for their valuable professional advice and suggestions. I also appreciate that I could always count on them as friends.

I extend my gratitude to my direct colleagues with whom I had the pleasure of working at the Institute of Laboratory Medicine and the János Szentágothai Research Centre.

Finally, I would like to deeply thank my mother, my partner, and my entire family for their support which made my studies possible. I am thankful for their understanding, help, and patience, without which this dissertation would not have been completed.